Electrical Characterization of Diamond/Boron Doped Diamond Nanostructures for Use in Harsh Environment Applications

To cite this article: Ł. Gołuński *et al* 2016 *IOP Conf. Ser.: Mater. Sci. Eng.* **104** 012022

IOP Conf. Series: Materials Science and Engineering **104** (2015) 012022 doi:10.1088/1757-899X/104/1/012022

Electrical Characterization of Diamond/Boron Doped Diamond Nanostructures for Use in Harsh Environment Applications

Ł. Gołuński[1,3], K. Zwolski[2], P. Płotka[2],

[1] Department of Metrology and Optoelectronics; Faculty of Electronics Telecommunication and Informatics; Gdańsk University of Technology; Gdańsk; Poland.
[2] Department of Microelectronic Systems; Faculty of Electronics Telecommunication and Informatics; Gdańsk University of Technology; Gdańsk; Poland.
[3] Faculty of Physics & Astronomy Physics; University of California, Riverside; Riverside; California, USA.

E-mail: lukgolun@student.pg.gda.pl

Abstract. The polycrystalline boron doped diamond (BDD) shows stable electrical properties and high tolerance for harsh environments (e.g. high temperature or aggressive chemical compounds) comparing to other materials used in semiconductor devices. In this study authors have designed electronic devices fabricated from non-intentionally (NiD) films and highly boron doped diamond structures. Presented semiconductor devices consist of highly boron doped structures grown on NiD diamond films. Fabricated structures were analyzed by electrical measurements for use in harsh environment applications. Moreover, the boron-doping level and influence of oxygen content on chemical composition of diamond films were particularly investigated. Microwave Plasma Enhanced Chemical Vapour Deposition (MW PE CVD) has been used for thin diamond films growth. Non-intentionally doped diamond (0 ppm [B]/[C]) films have been deposited on the Si/SiO_2 wafers with different content of carbon, boron and oxygen in the gas phase. Then, the shape of the highly doped diamond structures were obtained by pyrolysis of SiO_2 on NiD film and standard lithography process. The highly doped structures were obtained for different growth time and [B]/[C] ratio (4000 - 10000 ppm). The narrowest distance between two highly doped structures was 5µm. The standard Ti/Au ohmic contacts were deposited using physical vapour deposition for electrical characterization of NiD/BDD devices. The influence of diffusion boron from highly doped diamond into non-doped/low-doped diamond film was investigated. Surface morphology of designed structures was analyzed by Scanning Electron Microscope and optical microscope. The resistivity of the NiD and film was studied using four-point probe measurements also DC studies were done.

1. Introduction

Diamond shows unique electrical, physical, chemical and mechanical properties [1–3]. Due to its properties has many applications in electronics [2–7], MEMS [8–11], bio-sensors [12], may also act as an electromechanical sensor [13–15], be used for microfluidics [16] or be applied in neuron electrodes [11]. The chemical inertness of the polycrystalline boron doped diamond (BDD) combined with its high thermal conductivity, mechanical strength and electrical conductivity, makes it an attractive material for harsh environment applications.

The characterization of the electrical properties is of importance in order to be able to control and utilize diamond as an electronic material. In order to be able to characterize diamond thin films a new electronic devices have been designed. This devices have been fabricated from non-intentionally doped (NiD) diamond thin films and highly boron doped structures.
The NiD films and BDD structures has been grown by Microwave Plasma Enhanced Chemical Vapor Deposition (MW PE CVD). NiD films have been deposited on the Si/SiO_2 wafers. For the production diamond layers on Si/SiO_2 wafers, nucleation is necessary [1,3,17–19]. The most common used nucleation method is mechanical seeding of the substrate in water solution [19,20] or DMSO [21] with the use of ultrasound bath [22,23]. There are also known methods in which a thin film with nuclei is applied on a substrate [3]. In this methods the nanodiamond powder is placed in polyvinyl alcohol (PVA) matrix [24] or photoresist [25]. Based on diamond suspension technique in polymer PVA mixture [26] has been used for nucleation. This method is easy to obtain and in the PVA are elements only appearing during diamond synthesis by microwave plasma (H, C, O).
Highly boron doped structures has been fabricated by growing BDD structures on the NiD layer by method called second grown [27–29]. The second grown was successfully used for diamond growth [16,30]. For obtain shape of highly doped diamond structures (boxes in 4 size with different distance between them) a pyrolysis of SiO_2 on NiD film and standard lithography process has been used. Deposition and etching SiO_2 were exanimated by Smirnov et al [31].
In this paper authors investigated and showed influence of diffusion boron from highly doped diamond into non-doped/low-doped diamond film. The influence of diffusion has been shown by comparison resistivity of non-doped diamond layer measured by using four-point probe and V/I characteristics of non-doped/boron doped diamond structures. Also, morphology of designed structure was analyzed by Scanning Electron Microscope (SEM) and optical microscope.

2. Experimental

2.1.Growth of structure

Before growth diamond Si/SiO_2 (400nm thick SiO_2 by wet thermal oxidation) wafers have been rinsed in acetone and 2-isopropanol for 10 minutes in ultrasonic bath. After cleaning substrates have been dried in nitrogen blow. For nucleation PVA mixture with nanodiamonds was spin-coated on SiO_2 surface. The method of obtaining PVA mixture was described elsewhere [26,32]. NiD diamond layers 400nm thick were grown by µPA CVD system (SEKI 5250). Before process movable stage with samples was heated to 700°C. Temperature during deposition where increase by plasma heating up to 1000°C. The mixture of gases CH_4, H_2 and B_2H_6 was used to growth diamond. The NiD layer was grown with flow of gases H_2 - 298.5 sccm, CH_4 - 3 sccm, O_2 - 1 sccm . Gas pressure in the chamber were around 50 torr, and plasma were activated by microwaves 2.45 GHz at power 1300 W.
The SiO_2 mask on NiD diamond layer was obtained, for that at first, a layer of SiO_2 and thickness 1.5 µm was produced by pyrolytic method. In to the system (PCVD: Oxford Plasmalab System 80 Plus) a mixture of Si_2H_4 and N_2O was inserted in the ratio 1:5 with entire flow of 1200 sccm. SiO_2 deposition process was carried out in the temperature of 350°C, pressure of 1.5 torr and microwave power of 80W. The SiO_2 growth rate with those parameters is 169nm/min. . Next, on the NiD layer the photoresist was spin coated and exposed to UV light for 25s (Karl Suss Model MA-6.). In the next step, SiO_2 was etched by buffered oxide etch (BOE) 6:1.
Etched samples go back again to µPACVD system for one hour secondary growth of highly doped diamond structures. The structures were grown with 4000 and 10000 ppm [B]/[C] ratio. After second growth of diamond the Ohmic (Ti/Au) contacts were deposited on diamond structures by thermal evaporator (Temescal BJD 1800).

2.2. Analysis of structures

The NiD thin films were analysis by spectroscopic elipsometry and 4-point probe. For determining properties of continuous diamond layer on Si/SiO_2 substrate was used Jobin-Yvon UVISEL ellipsometer (HORIBA Jobin-Yvon Inc.). The investigated wavelength range was 260–830 nm. The experiments were performed at room temperature using an angle of incidence fixed at 70°. Ellipsometric fitting was based on a four-phase optical model roughness/diamond/SiO2/Si-wafer), Elipsometry were also used also for thickness analysis of SiO_2.

The morphology of obtained highly doped diamond structures (size of crystals and continuity) was determined by optical microscope (mikroLAB MMT 120 BT) and scanning electron microscope (SEM Hitachi S-3400N). Apart from that, SEM was used to analyze the highly doped structures, to assess smoothness of the edge lines, density of diamond grains occurrence within the areas of unintentional growth. Smoothness of the diamond phase edge was determined from SEM picture after graphic processing in GIMP programme (v. 2.6.11, GIMP development team) and a curve separating diamond and non-diamond phase was determined. As the y-axis was used a line parallel to expected direction of the edge line and contacting in a specific distance the smallest value of the curve. Next, the area under the curve was integrated and divided a segment length on which it was measured. The result was averaged for 10 segments of length 30 μm.

The surface resistivity of non-doped diamond layer was measured by 4-point probe connected to Keithley 2400 and computer with dedicated software. The conductivity between structures were measured by metallic needles on micromanipulators also connected to the Keithley 2400. The 4 point probe were used to analysis resistivity of diamond layer. In case when the film thickness is much smaller than the distance between the probes, the surface resistivity can be calculated from Eq:

$$\rho = \frac{\pi}{\ln(2)} \cdot \frac{V}{I} \cdot h \cdot f_2$$

where V is voltage measured on the internal probes, I is current applied to the external probes, h is the thickness of a layere and f_2 is correction factor [33]. The size of samples (20 mm x 20 mm) and spacing between probes (1.5 mm) gives value on correction factor around 0.97 [34].

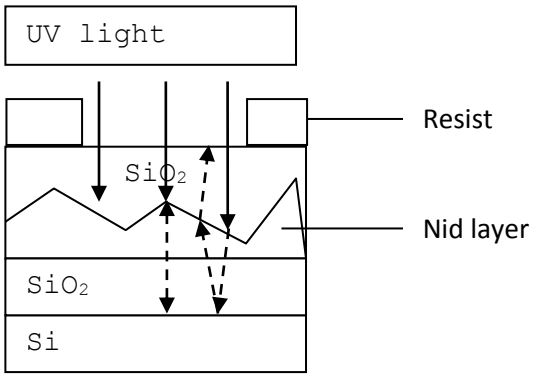

Figure 1. Imaging of contact UV light to not perpendicular surface of diamond.

3. Results and discussion

In the experiment the highly doped diamond structures in shape of pads with minimal size of 50μm were obtained. The NiD diamond layers were used as a substrate for second growth were obtained on Si/SiO_2 wafer with density of diamond nuclei $10^{10}/cm^2$. The thickness of diamond film was measured by elipsometry and was 300 nm which results growth rate of 5 nm/min.

To fabricate the SiO_2 mask for creating diamond structures was necessary to create SiO_2 layer on diamond. For the next step of production structures the 1.5 µm SiO_2 has been grown. For fabrication mask typical process of photolitography has been done. In reason of changed reflection by diamond from the background (figure 1) (compared to bare Si/SiO_2) to get high quality smooth mask from SiO_2 was necessary to change times exposition to UV light. Additional layers and also not flat diamond layer provides to longer way of the light and different intensity of exposition on some areas on sample. To decrease this negative effects it`s possible to increase the time of exposition to UV light. Good effect was obtained when Si/SiO_2/diamond/ SiO_2/photoresist sample was 3 times longer exposed to UV light than normally Si/SiO_2 structure. The differences of SiO_2 edged after short can be observed on figure 2.

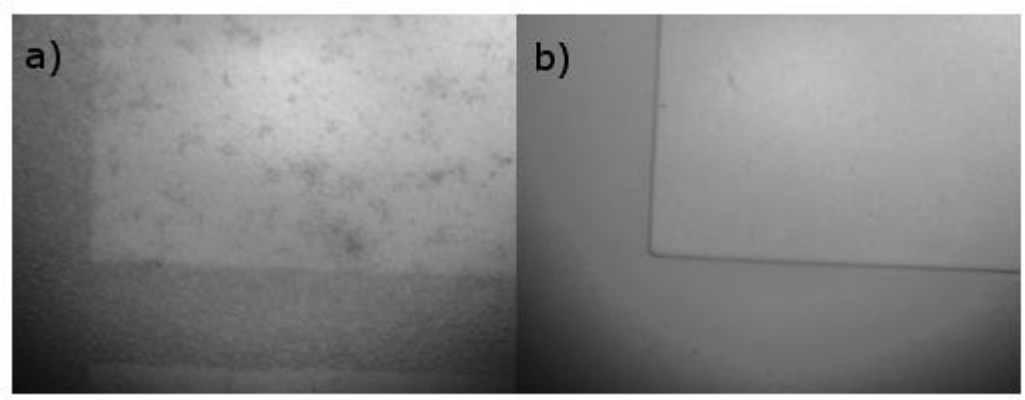

Figure 2. The shape of SiO_2 layer after etching with a) standard time of exposition to UV light (7 s) b) 3 times longer (21 s) exposition to UV light.

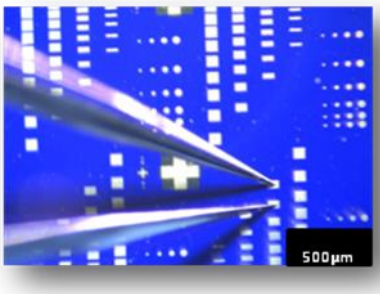

Figure 3. Obtained pads with cover Ti/Au picture from optical microscope.

Created and measured highly doped structures were in the shape of the pads in four sizes (50 x 200 µm, 100 x 200 µm, 150 x 200 µm and 200 x 200 µm). The pads of one size were put in the row and distance between them were increasing. The distance between next pads was starting from 5 µm from edge to edge goes by 10, 15, 20, 40, 60, 80, 100, 150 up to 200 µm (figure 3).
The SEM observations after NiD overgrowth by highly doped diamond structures show high quality edges. The amount of nuclei on the area of unintentional growth was close to 0. The minimal amount of crystals which were grown on black area in figure 4 have minor influence on the isolation between structures. Also the average smoothness of edge line was only 170 nm with maximum inclination of 500nm.
The Ohmic contacts has been used to get better contact to diamond layer in both cases to measured the surface resistivity of NiD layer and to measured contact between highly boron doped structures. The measured value of voltage at the minimum range of current were over the scale of measurement system shows that the material is an isolator.

The measured I/V characteristics have been done between every neighboring pads. The analyzed resistance between all pads of the same size shows almost linear changing resistivity to the distance

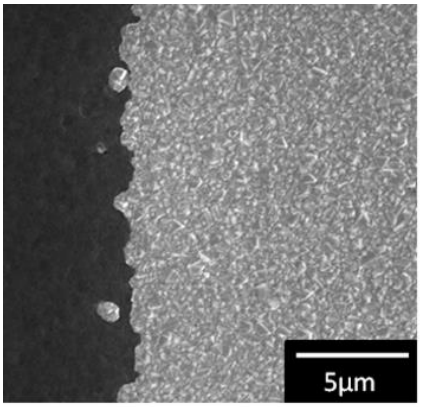

Figure 4. SEM of observed edge line with one of the crystals on non intentionaly phase growth.

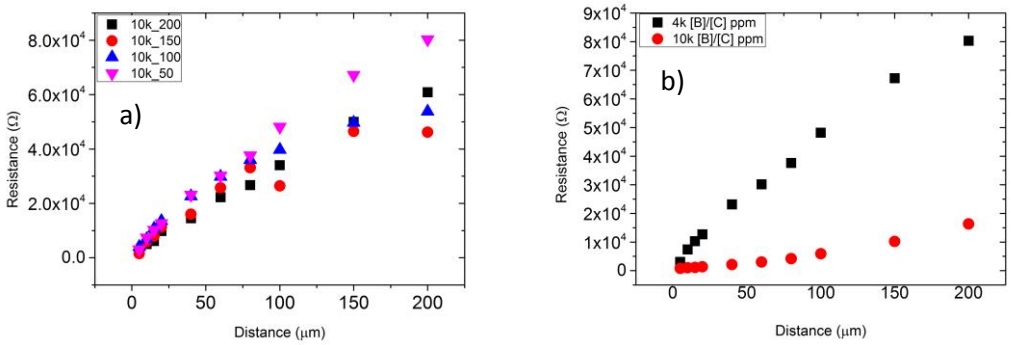

Figure. 5. (a) Comparison of resistance between different size pads (b) Resistivity comparison for two different level of dopant at pads of size 50 x 200 µm.

what was suspected. For small distances value of the resistance of all size pads it`s almost that same 6.5 x 10^3 Ω +/- 10^3 for 10 µm. The analysis the resistivity when distance is 150 µm the differences between pads are bigger and there are 5 x 10^4 Ω +/- 1.5 x 10^4. But it is impossible to recognize the influence of pads size on the resistivity (see figure 5). When compare all results it is possible to observe that using 10000 ppm [B]/[C] level of doping substrate you get better conductivity between the structures than when using 4000 ppm [B]/[C] in gas phase. The 4000 ppm level of doping has always 5 times bigger resistivity than 10000 ppm. It shows that some number of dopant migrate to the non-doped layer provides electrical contact between structures. This effect can be used by controlling the level of dopant migrating into NiD layer or low resistivity layer to build semiconductor devices.

4. References

[1] Butler J E and Sumant A V 2008 The CVD of Nanodiamond Materials *Chem. Vap. Depos.* **14** 145–60
[2] Geis M W, Twichell J C and Lyszczarz T M 1996 Diamond emitters fabrication and theory *J. Vac. Sci. Technol. B* **14** 2060–7
[3] Liu H and Dandy D S 1995 Studies on nucleation process in diamond CVD: an overview of recent developments *Diam. Relat. Mater.* **4** 1173–88
[4] Aleksov A, Kubovic M, Kaeb N, Spitzberg U, Bergmaier A, Dollinger G, Bauer T, Schreck M, Stritzker B and Kohn E 2003 Diamond field effect transistors—concepts and challenges *Diam. Relat. Mater.* **12** 391–8

[5] Kang W P, Davidson J L, Wisitsora-at A, Wong Y M, Takalkar R, Subramania K, Kerns D V and Hofmeister W H 2005 Diamond and carbon-derived vacuum micro- and nano-electronic devices *Diam. Relat. Mater.* **14** 685–91
[6] Gimenez S P 2010 Diamond MOSFET: An innovative layout to improve performance of ICs *Solid-State Electron.* **54** 1690–6
[7] Kang W P, Davidson J L, Wong Y M and Holmes K 2004 Diamond vacuum field emission devices *Diam. Relat. Mater.* **13** 975–81
[8] Sullivan J p., Friedmann T a. and Hjort K 2001 Diamond and Amorphous Carbon MEMS *MRS Bull.* **26** 309–11
[9] Luo J K, Fu Y Q, Le H R, Williams J A, Spearing S M and Milne W I 2007 Diamond and diamond-like carbon MEMS *J. Micromechanics Microengineering* **17** S147
[10] Hees J, Heidrich N, Pletschen W, Sah R E, Wolfer M, Williams O A, Lebedev V, Nebel C E and Ambacher O 2013 Piezoelectric actuated micro-resonators based on the growth of diamond on aluminum nitride thin films *Nanotechnology* **24** 025601
[11] Varney M W, Aslam D M, Janoudi A, Chan H-Y and Wang D H 2011 Polycrystalline-Diamond MEMS Biosensors Including Neural Microelectrode-Arrays *Biosensors* **1** 118–33
[12] Nebel C E, Rezek B, Shin D, Uetsuka H and Yang N 2007 Diamond for bio-sensor applications *J. Phys. Appl. Phys.* **40** 6443
[13] Bogdanowicz R, Czupryniak J, Gnyba M, Ryl J, Ossowski T, Sobaszek M, Siedlecka E M and Darowicki K 2013 Amperometric sensing of chemical oxygen demand at glassy carbon and silicon electrodes modified with boron-doped diamond *Sens. Actuators B Chem.* **189** 30–6
[14] Fabiańska A, Bogdanowicz R, Zięba P, Ossowski T, Gnyba M, Ryl J, Zielinski A, Janssens S D, Haenen K and Siedlecka E M 2013 Electrochemical oxidation of sulphamerazine at boron-doped diamond electrodes: Influence of boron concentration *Phys. Status Solidi A* **210** 2040–7
[15] Qureshi A, Kang W P, Davidson J L and Gurbuz Y 2009 Review on carbon-derived, solid-state, micro and nano sensors for electrochemical sensing applications *Diam. Relat. Mater.* **18** 1401–20
[16] Müller R, Schmid P, Munding A, Gronmaier R and Kohn E 2004 Elements for surface microfluidics in diamond *Diam. Relat. Mater.* **13** 780–4
[17] Lifshitz Y, Lee C H, Wu Y, Zhang W J, Bello I and Lee S T 2006 Role of nucleation in nanodiamond film growth *Appl. Phys. Lett.* **88** 243114
[18] Gruen D M 1999 Nanocrystalline Diamond Films1 *Annu. Rev. Mater. Sci.* **29** 211–59
[19] Williams O A, Douhéret O, Daenen M, Haenen K, Ōsawa E and Takahashi M 2007 Enhanced diamond nucleation on monodispersed nanocrystalline diamond *Chem. Phys. Lett.* **445** 255–8
[20] Varga M, Ižák T, Kromka A, Veselý M, Hruška K and Michalka M 2012 Study of diamond film nucleation by ultrasonic seeding in different solutions *Open Phys.* **10** 218–24
[21] Chu Y-C, Tu C-H, Jiang G, Chang C, Liu C, Ting J-M, Lee H-L, Tzeng Y and Auciello O 2012 Systematic studies of the nucleation and growth of ultrananocrystalline diamond films on silicon substrates coated with a tungsten layer *J. Appl. Phys.* **111** 124328
[22] Akhvlediani R, Lior I, Michaelson S and Hoffman A 2002 Nanometer rough, sub-micrometer-thick and continuous diamond chemical vapor deposition film promoted by a synergetic ultrasonic effect *Diam. Relat. Mater.* **11** 545–9
[23] Bogdanowicz R, Śmietana M, Gnyba M, Gołunski Ł, Ryl J and Gardas M 2014 Optical and structural properties of polycrystalline CVD diamond films grown on fused silica optical fibres pre-treated by high-power sonication seeding *Appl. Phys. A* **116** 1927–37
[24] Siuzdak K, Bogdanowicz R, Sawczak M and Sobaszek M 2014 Enhanced capacitance of composite TiO2 nanotube/boron-doped diamond electrodes studied by impedance spectroscopy *Nanoscale* **7** 551–8
[25] Wang M, Zhou Y S, Xie Z Q, Gao Y, He X N, Jiang L and Lu Y F 2013 Seed-Free Growth of Diamond Patterns on Silicon Predefined by Femtosecond Laser Direct Writing *Cryst. Growth Des.* **13** 716–22
[26] Scorsone E, Saada S, Arnault J C and Bergonzo P 2009 Enhanced control of diamond nanoparticle seeding using a polymer matrix *J. Appl. Phys.* **106** 014908
[27] Nishizawa J, Plotka P and Kurabayashi T 2002 Ballistic and tunneling GaAs static induction transistors: nano-devices for THz electronics *IEEE Trans. Electron Devices* **49** 1102–11
[28] Nishizawa J, Płotka P and Kurabayashi T 2008 GaAs area-selective regrowth with molecular layer epitaxy for integration of low noise and power transistors, and Schottky diodes *Phys. Status Solidi C* **5** 2799–801

[29] Nishizawa J, Oyama Y, Plotka P and Sakuraba H 1996 Optimization of low temperature surface treatment of GaAs crystal *Surf. Sci.* **348** 105–14
[30] Aharonovich I, Lee J C, Magyar A P, Buckley B B, Yale C G, Awschalom D D and Hu E L 2012 Homoepitaxial Growth of Single Crystal Diamond Membranes for Quantum Information Processing *Adv. Mater.* **24** OP54–9
[31] Smirnov W, Yang N, Hoffmann R, Hees J, Obloh H, Müller-Sebert W and Nebel C E 2011 Integrated All-Diamond Ultramicroelectrode Arrays: Optimization of Faradaic and Capacitive Currents *Anal. Chem.* **83** 7438–43
[32] Bogdanowicz R, Fabiańska A, Golunski L, Sobaszek M, Gnyba M, Ryl J, Darowicki K, Ossowski T, Janssens S D, Haenen K and Siedlecka E M 2013 Influence of the boron doping level on the electrochemical oxidation of the azo dyes at Si/BDD thin film electrodes *Diam. Relat. Mater.* **39** 82–8
[33] Schroder D K 2006 *Semiconductor Material and Device Characterization* (John Wiley & Sons)
[34] Smits F M 1958 Measurement of sheet resistivities with the four-point probe *Bell Syst. Tech. J.* **37** 711–8

Acknowledgments
The authors gratefully acknowledge financial support from the Polish National Science Centre (NCN) under grant no. 2011/03/D/ST7/03541 and 2014/14/M/ST5/00715. The DS funds of the Faculty of Electronics, Telecommunications and Informatics of the Gdansk University of Technology are also acknowledged